THE JOURNAL OF PHYSICAL CHEMISTRY A

Article

pubs.acs.org/JPCA

Gas-Phase Synthesis and Structure of Monomeric ZnOH: A Model Species for Metalloenzymes and Catalytic Surfaces

Lindsay N. Zack,[†] Ming Sun,[†,‡] Matthew P. Bucchino,[†] Dennis J. Clouthier,[§] and Lucy M. Ziurys*[,†]

[†]Department of Chemistry, Department of Astronomy and Steward Observatory, University of Arizona, 933 North Cherry Avenue, Tucson, Arizona 85721, United States

[§]Department of Chemistry, University of Kentucky, 125 Chemistry-Physics Building, Lexington, Kentucky 40506, United States

Supporting Information

ABSTRACT: Monomeric ZnOH has been studied for the first time using millimeter and microwave gas-phase spectroscopy. ZnOH is important in surface processes and at the active site of the enzyme carbonic anhydrase. In the millimeter-wave direct-absorption experiments, ZnOH was synthesized by reacting zinc vapor, produced in a Broida-type oven, with water. In the Fourier-transform microwave measurements, ZnOH was produced in a supersonic jet expansion of CH_3OH and zinc vapor, created by laser ablation. Multiple rotational transitions of six ZnOH isotopologues in their X^2A' ground states were measured over the frequency range of 22−482 GHz, and splittings due to fine and hyperfine structure were resolved. An asymmetric top pattern was observed in the spectra, showing that ZnOH is bent, indicative of covalent bonding. From these data, spectroscopic constants and an accurate structure were determined. The Zn−O bond length was found to be similar to that in carbonic anhydrase and other model enzyme systems.

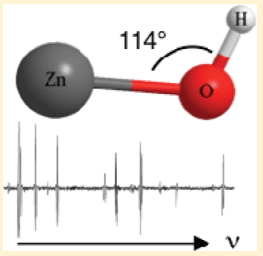

INTRODUCTION

Zinc-containing molecules are known to exhibit unusual chemical properties, making them useful compounds in catalysis, surface science, nanotechnology, and biological processes; e.g., see refs1−3. One particular species of interest in this regard is the simple triatomic molecule, ZnOH, often written as Zn^+OH^-. For example, the ZnOH unit and its hydrated form, $Zn(H_2O)$, are present in thousands of enzymes and proteins; e.g., see refs 4 and 5. Carbonic anhydrase (CA), an enzyme that catalyzes the hydration of CO_2, is one of the most studied zinc hydroxide-containing biological molecules. The catalytic site of CA is based on tetrahedrally coordinated zinc, with three histidine units as ligands and the fourth either a water molecule or hydroxide, depending on the pH environment (Figure 1a). It is thought that the ZnOH unit, a strong nucleophile, is the vehicle for attack on the substrate, in this case CO_2.[4] ZnOH thus plays a critical role in the enzyme function of CA.

The catalytic site in Zn-bearing enzymes has been studied by a variety of experimental and theoretical methods. In most cases, a L_3Zn-OH or tripod-ZnOH complex has been used as a model system to determine reaction mechanisms;[6−10] see Figure 1b. This type of work has been carried out mostly in the liquid phase; however, gas-phase studies have also been conducted. During these reactions, structural information, such as the Zn−O bond distance, has also been obtained via X-ray crystallography, although the exact geometry of the ZnOH unit is not known. The energetics and structure of these systems have been modeled at various levels of theory, as well, including ab initio, molecular dynamics, and density functional theory (DFT) calculations.[11−14] Such studies have shown that the key property of the ZnOH unit in enzyme activity is a rapid change in coordination number and geometry at the metal center.[6]

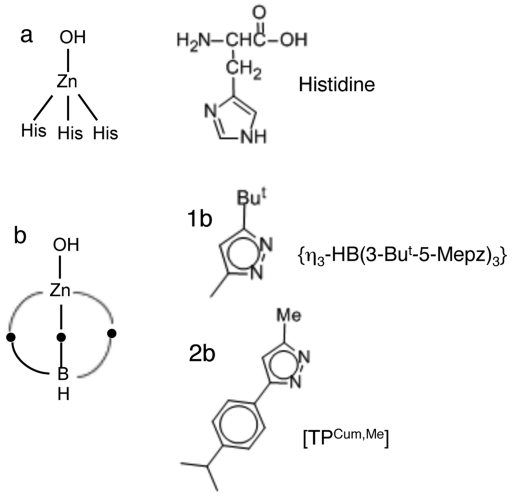

Figure 1. (a) Structures of the carbonic anhydrase (CA) active site, which contain a ZnOH unit bonded to three histidine units. (b) Example model systems for CA, featuring bulky tripod ligands, which mimic the structure of the active site of the enzyme.

In addition to its importance in biochemistry and enzymology, ZnOH has been shown to play a significant role in surface chemistry. For example, the formation of ZnOH groups on zeolites provides acidic sites where alkane activation

Received: October 13, 2011
Revised: January 6, 2012
Published: January 9, 2012

and dehydrogenation reactions can occur,[15,16] making these regions useful for catalysis. Corrosion studies have also focused on the formation of ZnOH by the reaction of Zn/ZnO surfaces with water. Under atmospheric conditions, it has been shown that the OH group and formic acid undergo ligand exchange at the zinc center, adding further corrosive effects on a given surface.[2]

From a basic chemistry viewpoint, studies of ZnOH and similar 3d species give insight into properties of metal−OH bonds across the periodic table. To date, numerous measurements have been made of the gas-phase spectra of alkali and alkaline earth monohydroxide molecules.[17−24] These species exhibit linear or quasilinear structures, depending on whether the metal−oxygen bond is highly ionic (linear) or ionic with some covalent character (quasilinear). Group 13 metals tend to form bonds with -OH that have a high degree of covalent character, exhibiting bent or quasilinear geometries.[25] It should be noted that the simplest monohydroxide species, H_2O, is bent with a bond angle ∼104°, indicating a true covalent structure with sp^3 hybridization at the oxygen atom. Transition metal monohydroxides, on the other hand, have not been well characterized. Only YOH, AgOH, and CuOH have been studied in any detail, although a recent molecular beam investigation, using time-of-flight mass spectrometry (TOF-MS), has identified ZnOH as a reaction product of laser-ablated zinc metal and water.[26] The electronic spectrum of YOH clearly shows the pattern of a linear molecule,[27] while both CuOH and AgOH are bent.[28] This difference in geometry indicates that significant changes in bonding occur across the transition metal series, but more data are clearly needed.

Studies of metal monohydroxide species, including ZnOH, have also been pursued in the solid phase, usually by examining the reaction products of metals or metal ions with water in an argon matrix. Although metal monohydroxides are produced, these reactions typically result in the formation of HMOH insertion products[29,30] or $M(OH)_2$ adducts.[31] Interestingly, CuOH and ZnOH were also seen in matrices upon photolysis,[29,31] despite having unfavorable heats of formation.[29]

The metal 3d MOH series has also been the topic of theoretical investigations. In 2001, Trachtman et al. carried out ab initio calculations on several metal monohydroxide species at the MP2 and CCSD levels, determining bond lengths and bond angles.[32] Magnusson and Moriarty[33] have examined binding energies of both singly and doubly charged transition metals with different ligands. They found that the binding energies for transition metal ions with OH^- are larger than with H_2O. These authors suggest that this difference arises from better orbital overlap of the hydroxide ligand (OH^-) with the 4s orbital of the metal ion than with the aqua ligand (H_2O). Thus, the OH^- group is less shielded from the nucleus and can form a stronger bond.[33] Moreover, many MOH species are thought to have C_s symmetry, so the energy surface can be minimized by changes in bond angle.

In this paper, we present the first gas-phase structural characterization of monomeric ZnOH, as determined by high-resolution rotational spectroscopy. Millimeter/sub-millimeter−wave direct−absorption techniques and Fourier-transform microwave (FTMW) methods have been used to study this radical in its ground X^2A' electronic state. Rotational transitions of six isotopologues of the molecule were recorded in multiple K_a asymmetry components; spin rotation and hyperfine splittings were also observed, the latter arising from the hydrogen nuclear spin (I = 1/2). From these data, the first accurate structure of the free ZnOH unit has been determined. Insight into the orbital composition of the unpaired electron has also been obtained. Here we present our data and analysis for ZnOH and discuss their chemical implications.

EXPERIMENTAL METHODS

The rotational spectra of six ZnOH isotopologues (^{64}ZnOH, ^{66}ZnOH, ^{68}ZnOH, ^{64}ZnOD, ^{66}ZnOD, and ^{68}ZnOD) were recorded using a millimeter/sub-millimeter direct-absorption spectrometer of the Ziurys group, described in detail elsewhere.[34] In this spectrometer, tunable millimeter-wave radiation is produced by Gunn oscillators in combination with Schottky diode multipliers. The radiation is quasi-optically focused through a double-pass reaction chamber containing a Broida-type oven and then directed into a helium-cooled, InSb hot-electron bolometer detector. Several lenses (two of which seal the reaction cell), a rooftop reflector, and a polarizing grid direct the radiation through the spectrometer system. Phase-sensitive detection is achieved by modulating the source at 25 kHz and detecting signals at 2f with a lock-in amplifier.

In this spectrometer, the ZnOH radical was synthesized by reacting zinc vapor with either H_2O or 30% H_2O_2 in the presence of a 250 mA direct current (dc) discharge. Metal vapor was produced by melting zinc pieces (99.9%, Aldrich) in an alumina crucible using a Broida-type oven. Production was maximized when roughly 2−3 mTorr of H_2O was added over the top of the oven, while argon carrier gas was introduced underneath the oven heating unit. Because zinc has a tendency to coat the optics, greatly attenuating any signals, argon gas was also flowed over the lenses at both ends of the reaction chamber. Altogether, the pressure in the cell due to argon was approximately 15 mTorr. Production of ZnOD was achieved by replacing H_2O with D_2O (99.9% D, Cambridge Isotope Laboratories).

Precise transition frequencies were determined by fitting Gaussian curves to line profiles, obtained from averaging an equal number of scans in increasing and decreasing frequency, each of which had a 5 MHz scan width. For weaker features, up to 12 scan pairs were needed in order to obtain a sufficient signal-to-noise ratio. Typical line widths ranged from around 0.6 to 1.5 MHz over the frequency range of 200−482 GHz for unblended features. The instrumental accuracy is estimated to be ±50 kHz.

Spectra of two isotopologues, ^{64}ZnOH and ^{66}ZnOH, were measured using the Fourier-transform microwave (FTMW) spectrometer of the Ziurys' group.[35] The instrument is a Balle−Flygare type[36] narrow-band spectrometer consisting of a vacuum chamber with an unloaded pressure of ∼10^{-8} Torr, maintained by a cryopump. The chamber is a Fabry−Perot cavity consisting of two spherical aluminum mirrors in a near confocal arrangement, with an antenna embedded in each mirror: one for injecting the microwave signal and the other for detecting the resulting molecular emission. Precursor gases are introduced into the chamber using a pulsed-valve nozzle (General Valve) aligned 40° relative to the mirror axis. The nozzle is equipped with a laser ablation/dc discharge source. The laser is a Surelite I-10 Nd:YAG laser operated at the second harmonic (532 nm) and run at a repetition rate of 10 Hz with 100 mJ/pulse.[37] The signals are recorded in the time domain with an instantaneous bandwidth of 600 kHz, before being fast Fourier-transformed to create a frequency-domain spectra with 2 kHz resolution. Each transition appears as a Doppler doublet with a full width at half-maximum (FWHM)

dx.doi.org/10.1021/jp209875a | J. Phys. Chem. A 2012, 116, 1542−1550

of 5 kHz per feature, and the rest frequencies are simply taken as the average of the two components.

In the FTMW spectrometer, the ZnOH radical was synthesized in a supersonic jet expansion from a mixture of 0.5% methanol in argon and zinc vapor, produced from the ablation of a Zn rod. The mixture was passed through a dc discharge before entering the cavity. The gas-pulse duration was set to 550 μs, creating a 40−60 cm^3(STP) min^{-1} mass flow at a backing pressure of 45 psi. The ZnOH signal was maximized at a discharge voltage of 1100 V at 50 mA. Several nozzle pulses, or "shots", were necessary to achieve adequate signal-to-noise ratios. For ^{64}ZnOH, 250 shots were needed, while ^{66}ZnOH required 500 shots.

RESULTS AND ANALYSIS

Theoretical studies have suggested a X^2A' electronic ground state for ZnOH,[32,33] i.e., a bent structure with C_s symmetry, and one unpaired electron. For this electronic term, the rotational levels are labeled by the quantum numbers N, K_a, and K_c. Spin-rotation coupling additionally splits the energy levels into two sublevels, which are labeled by the quantum number J, where $\mathbf{J} = \mathbf{N} + \mathbf{S}$. The spin-rotation interaction thus generates doublets. The largest dipole moment of ZnOH is along the a molecular axis. The favored transitions therefore follow the selection rules $\Delta N = \pm 1$, $\Delta J = \pm 1$, $\Delta K_a = 0$, and $\Delta K_c = \pm 1$.

Because no previous spectroscopic data existed for ZnOH, a continuous frequency range of approximately 70 GHz (~6 B_{eff}, where $B_{eff} = (B + C)/2$), based on theoretical predictions, was initially scanned with the millimeter-wave spectrometer.[32] Across this frequency range, several groups of doublets separated by ~185−200 MHz were observed, suggesting the presence of a zinc-containing molecule with a single unpaired electron. These groups of lines were found to be harmonically related, with an effective rotational constant of $B_{eff} \sim 11$ GHz, as predicted for ZnOH. A closer look at a single group of lines revealed three distinct clusters of features with a relative frequency spacing similar to the characteristic ^{64}Zn:^{66}Zn:^{68}Zn isotope pattern;[38−40] these groups had to arise from ^{64}ZnOH, ^{66}ZnOH, and ^{68}ZnOH. With this assignment, the pattern for a-type transitions of a near-prolate asymmetric rotor could then be identified for each isotopologue, beginning with the $K_a = 0$, 2, 3, and 4 asymmetry components. The $K_a = 1$ asymmetry components were more difficult to locate, as they were typically blended into the patterns of other isotopologues. The observed spin-rotation splittings, each characteristic of a given K_a value, also played a role in the assignment of asymmetry components. No b-type transitions were identified. The spectrum of ZnOD was assigned in a similar manner.

Stick spectra of all six isotopologues of ZnOH in the $N = 13 \rightarrow 14$ transition, observed with the millimeter-wave spectrometer near 280−300 GHz, are presented in Figure 2, with approximate intensities. All features are labeled by their K_a quantum number, and for simplicity, the spin-rotation splittings have been collapsed. These patterns, which vary somewhat with molecular mass, clearly indicate a bent molecule and illustrate the complex nature of the spectra. The shift of the $K_a = 0$ component to lower frequency for ZnOD, relative to its position in ZnOH, for example, indicates a higher degree of asymmetry for the deuterated species, as expected. Also, the asymmetry doubling for the $K_a = 1$ and 2 components of ZnOD is larger than that of ZnOH.

A representative millimeter-wave spectrum of a section of the $N = 20 \rightarrow 21$ transition of ^{68}ZnOH near 458 GHz is shown in Figure 3, observed in natural abundance (^{64}Zn:^{66}Zn:^{68}Zn = 48.6:27.9:18.8). The $K_a = 0$ and $K_a = 2$ asymmetry components are visible in the spectrum, labeled by K_a, with brackets showing the spin-rotation splitting of ~190 MHz. The $K_a = 2$ component shows clear asymmetry doubling.

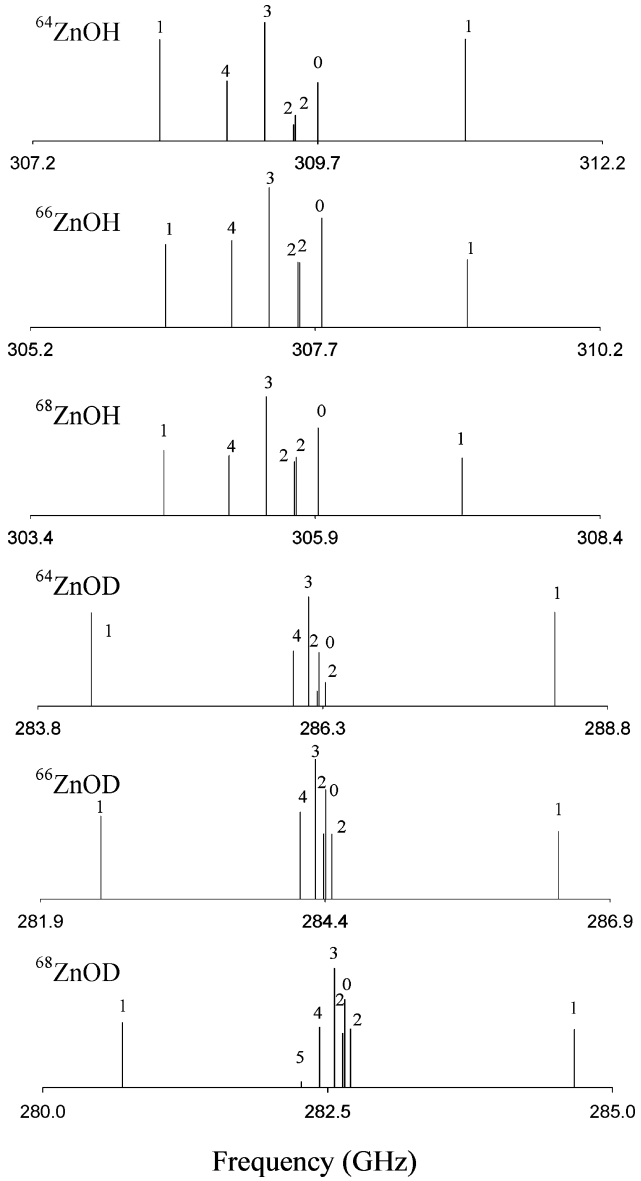

Figure 2. Stick figure showing the observed asymmetry components of the $N = 13 \rightarrow 14$ rotational transition of the six ZnOH isotopologues measured in this work at millimeter wavelengths, with approximate relative intensities. For simplicity, the spin-rotation doublets have been collapsed and the individual transitions are indicated by the K_a quantum number ($\Delta K_a = 0$).

In Figure 4, a section of the millimeter-wave spectrum of the $N = 18 \rightarrow 19$ transition of ^{64}ZnOD near 388 GHz is displayed, with lines arising from the $K_a = 0$, 2, 3, and 4 components. Spin rotation splittings, about 180 MHz in magnitude for this species, are indicated by brackets. Only one spin-rotation component of the $K_a = 4$ component is visible in this spectra; its pair is outside the displayed frequency range. The asymmetry splitting is collapsed in all of the components shown here, except for the $K_a = 2$ component, which exhibits an obvious doublet. A spin-rotation line arising from a $K_a = 1$ component of ^{66}ZnOD is also present.

dx.doi.org/10.1021/jp209875a | J. Phys. Chem. A 2012, 116, 1542−1550

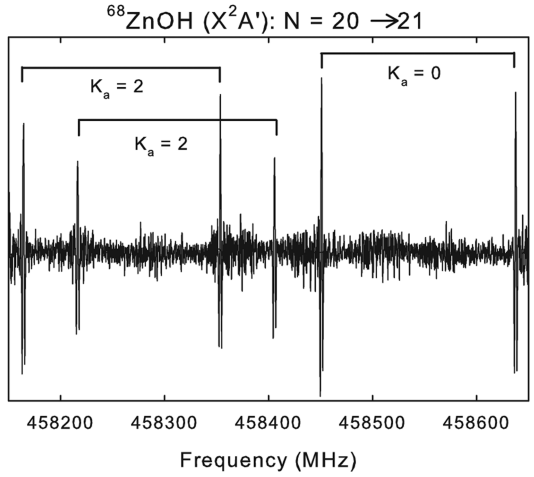

Figure 3. Spectra of a section of the $N = 20 \rightarrow 21$ transition of ^{68}ZnOH (in natural zinc abundance) near 458 GHz, measured by millimeter−wave direct−absorption methods. Shown here are the $K_a = 0$ and $K_a = 2$ asymmetry components, which are further split into spin-rotation doublets, indicated by brackets. The spectrum is a composite of five 100 MHz scans, each acquired in ∼60 s.

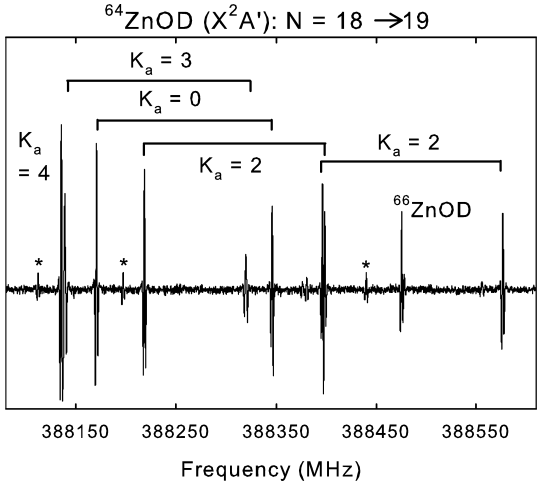

Figure 4. Section of the $N = 18 \rightarrow 19$ transition of ^{64}ZnOD near 388 GHz, also observed using millimeter−wave direct−absorption techniques. The transitions are labeled by K_a, and spin-rotation doublets are indicated by brackets. Here the $K_a = 0$, 2, 3, and 4 asymmetry components are displayed, with the $K_a = 2$ showing significant splitting. For the $K_a = 4$ line, one spin-rotation component lies outside the given frequency range. Also present in the spectrum is one of the $K_a = 0$ asymmetry components of ^{66}ZnOD. Unassigned lines are marked by asterisks. The spectrum is a composite of five 100 MHz scans, each acquired in ∼60 s.

Once the millimeter-wave spectra were assigned, the $N = 1 \rightarrow 0$ transitions were recorded for ^{64}ZnOH and ^{66}ZnOH using the FTMW spectrometer near 22 GHz. In these transitions, hyperfine splittings were observed, arising from the coupling of the nuclear spin of hydrogen (I(H) = 1/2) with the electron spin angular momentum, so-called **I**·**S** interactions. A sample FTMW spectrum for the $J = 1.5 \rightarrow 0.5$ spin component of the $N = 1 \rightarrow 0$, $K_a = 0$ transition of ^{64}ZnOH is shown in Figure 5. Here two hyperfine components are present, labeled by quantum number F, where $\mathbf{F} = \mathbf{I} + \mathbf{J}$. Doppler doublets, characteristic of FTMW data, are clearly visible in the $F = 2 \rightarrow 1$ line, the stronger hyperfine component. The weaker $F = 1 \rightarrow 0$ feature appears to be broader, likely due to a slight Zeeman effect caused by the Earth's magnetic field.

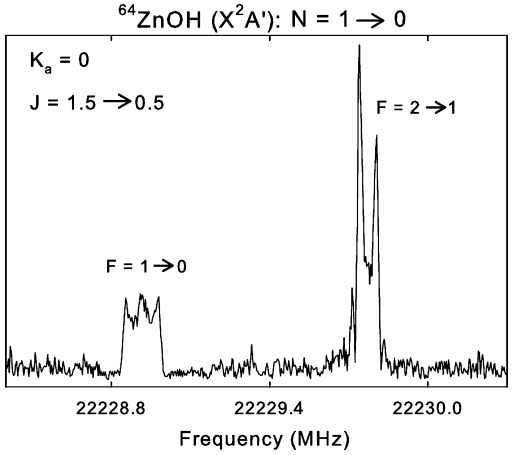

Figure 5. Spectrum of one spin-rotation component ($J = 1.5 \rightarrow 0.5$) of the $N = 1 \rightarrow 0$ transition of ^{64}ZnOH measured with the FTMW spectrometer near 22 GHz. In this case, only $K_a = 0$ lines exist. Two favorable hyperfine transitions are apparent in the data, arising from the H nucleus and labeled with the quantum number F. Each line is split into Doppler doublets. The $F = 1 \rightarrow 0$ feature appears somewhat broader due to a small Zeeman effect caused by the Earth's magnetic field This spectrum is an average of 500 pulses.

In total, 435 and 404 transition frequencies were measured for ZnOH and ZnOD, respectively. The microwave frequencies and a subset of millimeter-wave frequencies are shown in Table 1. (A complete table of millimeter−wave transition frequencies is available in the Supporting Information.) For each isotopologue, the spin-rotation doublets of the asymmetry components $K_a = 0$−4 were recorded in eight rotational transitions $N \rightarrow N + 1$ over the frequency range of 200−482 GHz. An additional transition ($N = 1 \rightarrow 0$) was measured for ^{64}ZnOH and ^{66}ZnOH. Asymmetry doubling was only observed in the $K_a = 1$ and 2 lines; however, at higher N, the $K_a = 3$ lines of ZnOD appeared broader than expected, indicative of such doubling.

The data for ZnOH and ZnOD were analyzed using the nonlinear least-squares code SPFIT,[41] with Watson's S-reduced asymmetric top model.[42] The effective Hamiltonian included terms for molecular frame rotation, centrifugal distortion, spin-rotation, and magnetic hyperfine interactions:

$$\mathbf{H}_{\mathrm{eff}} = \mathbf{H}_{\mathrm{rot}} + \mathbf{H}_{\mathrm{cd}} + \mathbf{H}_{\mathrm{sr}} + \mathbf{H}_{\mathrm{mhf}}(H) \qquad (1)$$

For the ZnOH isotopologues, 10 rotational parameters, including two sixth-order terms (H_{KN} and h_3), one eighth-order constant (L_{KKN}), and a tenth-order correction (P_{KN}), were needed to fit the data. Only nine rotational constants, up to the sixth order (H_{KN} and h_3), were necessary for the ZnOD species. The diagonal parameters ε_{aa}, ε_{bb}, and ε_{cc} of the spin-rotation tensor were included in the analysis, as well as a centrifugal distortion correction, D_N^S. The off-diagonal element of this tensor, $(\varepsilon_{ab} + \varepsilon_{ba})/2$, was also used in the ZnOD fits. For ^{64}ZnOH and ^{66}ZnOH, two hyperfine parameters, the Fermi contact constant a_F and T_{aa}, one of the diagonal terms of the dipolar tensor, were fit in the analysis, as well. The spectroscopic constants for the ZnOH species are presented in Table 2.

dx.doi.org/10.1021/jp209875a | J. Phys. Chem. A 2012, 116, 1542−1550

Table 1. Selected Rotational Transition Frequencies of ZnOH (X^2A') in Megahertz

											^{64}ZnOH		^{66}ZnOH		^{68}ZnOH		^{64}ZnOD	
N''	K_a''	K_c''	J''	F''		N'	K_a'	K_c'	J'	F'	ν_{obs}	$\nu_{obs-calc}$	ν_{obs}	$\nu_{obs-calc}$	ν_{obs}	$\nu_{obs-calc}$	ν_{obs}	$\nu_{obs-calc}$
0	0	0	0.5	0	←	1	0	1	0.5	1	21 942.798	−0.013						
0	0	0	0.5	1	←	1	0	1	0.5	1	21 946.954	−0.013						
0	0	0	0.5	0	←	1	0	1	1.5	1	22 228.916	−0.039	22 089.313	0.001				
0	0	0	0.5	1	←	1	0	1	1.5	2	22 229.773	0.003	22 090.169	0.003				
0	0	0	0.5	1	←	1	0	1	1.5	1	22 233.081	−0.013	22 093.480	0.001				
13	0	13	12.5		→	14	0	14	13.5		309 606.409	0.208	307 663.441	0.124	305 832.698	0.128	286 179.061	0.076
13	0	13	13.5		→	14	0	14	14.5		309 795.969	−0.086	307 851.807	−0.149	306 020.016	−0.123	286 354.814	−0.011
13	1	13	12.5		→	14	1	14	13.5		308 218.586	0.096	306 292.603	0.047	304 477.850	0.101	284 179.595	0.062
13	1	13	13.5		→	14	1	14	14.5		308 409.802	−0.049	306 482.660	−0.044	304 666.769	−0.059	284 356.262	−0.038
13	1	12	12.5		→	14	1	13	13.5		310 900.834	0.131	308 941.403	0.103	307 095.260	0.117	288 248.692	0.068
13	1	12	13.5		→	14	1	13	14.5		311 091.858	−0.046	309 131.247	−0.017	307 283.957	−0.078	288 425.774	−0.030
13	2	12	12.5		→	14	2	13	13.5		309 391.638	−0.035	307 450.571	−0.088	305 621.704	−0.030	286 160.524	−0.117
13	2	12	13.5		→	14	2	13	14.5		309 587.287	0.048	307 645.035	0.064	305 815.016	0.042	286 340.890	−0.072
13	2	11	12.5		→	14	2	12	13.5		309 407.845	−0.052	307 466.387	−0.094	305 637.157	<0.000	286 232.733	−0.106
13	2	11	13.5		→	14	2	12	14.5		309 603.516	0.056	307 660.819	0.029	305 830.474	0.080	286 413.101	−0.083
13	3	11	12.5		→	14	3	12	13.5		309 134.334	−0.097	307 195.796	−0.182	305 369.302	−0.060	286 082.675	−0.008
13	3	11	13.5		→	14	3	12	14.5		309 337.221	0.088	307 397.470	0.093	305 569.795	0.109	286 268.663	0.070
13	3	10	12.5		→	14	3	11	13.5		309 134.334	−0.113	307 195.796	−0.197	305 369.302	−0.075	286 082.675	−0.008
13	3	10	13.5		→	14	3	11	14.5		309 337.221	0.072	307 397.470	0.078	305 569.795	0.094	286 268.663	0.069
13	4	10	12.5		→	14	4	11	13.5		308 798.154	0.079	306 863.067	0.039	305 039.476	−0.140	285 944.768	0.030
13	4	10	13.5		→	14	4	11	14.5		309 010.628	−0.129	307 074.256	−0.083	305 249.742	−0.106	286 138.450	−0.006
13	4	9	12.5		→	14	4	10	13.5		308 798.154	0.079	306 863.067	0.039	305 039.476	−0.140	285 944.768	0.031
13	4	9	13.5		→	14	4	10	14.5		309 010.628	−0.129	307 074.256	−0.083	305 249.742	−0.106	286 138.450	−0.005

dx.doi.org/10.1021/jp209875a | J. Phys. Chem. A 2012, 116, 1542–1550

Table 2. Spectroscopic Constants for Isotopologues of ZnOH (X^2A')[a]

parameters	^{64}ZnOH	^{66}ZnOH	^{68}ZnOH	^{64}ZnOD	^{66}ZnOD	^{68}ZnOD
A	745 084(1800)	741 576(2200)	739 732(3100)	402 650(170)	402 623(180)	402 701(190)
B	11 163.4978(51)	11 092.7985(59)	11 026.1877(70)	10 377.237 8(54)	10 308.702 4(55)	10 244.132 7(55)
C	10 971.5173(51)	10 903.2201(55)	10 838.8526(69)	10 085.852 8(54)	10 021.089 1(55)	9 960.045 2(54)
D_N	0.015 6697(17)	0.015 4772(19)	0.015 2896(25)	0.013 0081(22)	0.012 841 2(23)	0.012 685 8(22)
D_{NK}	2.126 9(28)	2.111 2(34)	2.092 2(40)	0.708 13(47)	0.697 90(46)	0.688 09(44)
d_1	$-2.541(36) \times 10^{-4}$	$-2.473(35) \times 10^{-4}$	$-2.449(54) \times 10^{-4}$	$-4.498(45) \times 10^{-4}$	$-4.391(46) \times 10^{-4}$	$-4.309(46) \times 10^{-4}$
d_2	$-3.99(23) \times 10^{-5}$	$-4.25(26) \times 10^{-5}$	$-4.46(36) \times 10^{-5}$	$-6.30(21) \times 10^{-5}$	$-6.17(24) \times 10^{-5}$	$-5.96(22) \times 10^{-5}$
H_{KN}	0.0305 5(92)	0.0319(10)	0.031 9(12)	0.001 907(26)	0.001 881(25)	0.001 850(24)
h_3				$-3.60(74) \times 10^{-8}$	$-3.47(74) \times 10^{-8}$	$-3.34(42) \times 10^{-8}$
L_{KKN}	−0.001 06(10)	−0.00121(11)	−0.001 23(12)			
P_{KN}	$2.25(35) \times 10^{-5}$	$2.72(36) \times 10^{-5}$	$2.80(41) \times 10^{-5}$			
ε_{aa}	−86.86(57)	−86.21(74)	−87.11(75)	−40.81(72)	−40.39(73)	−40.93(74)
ε_{bb}	189.89(10)	188.63(11)	187.63(12)	176.42(12)	175.34(12)	174.22(12)
ε_{cc}	190.21(10)	188.99(11)	188.00(12)	175.62(12)	174.49(13)	173.37(12)
$(\varepsilon_{ab} + \varepsilon_{ba})/2$				14.2(2.3)	15.0(2.7)	14.1(3.4)
D_N^S	$-1.01(59) \times 10^{-6}$	$-8.87(59) \times 10^{-7}$	$-1.30(13) \times 10^{-6}$	$-8.4(1.2) \times 10^{-7}$	$-9.6(1.2) \times 10^{-7}$	$-7.8(1.1) \times 10^{-7}$
a_F (H)	−4.138(19)	−4.167(21)				
T_{aa} (H)	4.176(32)	3.95(14)				
Δ_0 (uÅ^2)	0.1138	0.1109	0.1090	0.1519	0.1519	0.1521
rms of fit	0.106	0.095	0.113	0.073	0.083	0.085

[a]In megahertz unless otherwise noted. Errors are 3σ statistical uncertainties to the last quoted digit.

Table 3. Structures for ZnOH and Similar Molecules[a]

	r_{MO} (Å)	r_{OH} (Å)	∠MOH (deg)	method
ZnOH	1.809(5)	0.964 (7)	114.1(5)	r_0
ZnOH[b]	1.795(1)	0.967(3)	114.2(2)	$r_m^{(1)}$
ZnOH[c]	1.817	0.962	114.9	theory: MP2
CAII[d]	2.05(6)			X-ray
[Tp^{Cum,Me}]ZnOH[e]	1.85(6)			X-ray
{η^3-HB(3-Bu^t-5-Mepz)$_3$}ZnOH[f]	1.85(6)			X-ray
[(NH$_3$)$_3$Zn(OH)]$^{+g}$	1.854		124.1	theory: DFT
ZnO[h]	1.704 7(2)			r_e
CuO[i]	1.729			r_0
CuOH[j]	1.771 82(3)	0.964 6(3)	110.12(30)	r_z
AgOH[j]	2.018 49(4)	0.963 9(1)	107.81(2)	r_z
YOH[k]	1.948 61(38)	0.920 6(34)	180.0	r_0
OH^{-l}		0.964 317(33)		r_e
HOH[m]		0.957 848(48)	104.542(14)	r_e

[a]3σ error. [b]Watson's parameters are c_a = −0.46(9), c_b = 0.10(7), and c_c = 0.11(7). [c]Reference 32. [d]Reference 49; 1.54 Å resolution. [e]Reference 50. [f]Reference 51. [g]Reference 14; B3LYP/6-311+G** level. [h]Reference 40. [i]Reference 48. [j]Reference 47. [k]Reference 27. [l]Reference 45. [m]Reference 46.

DISCUSSION

As mentioned previously, very ionic metal monohydroxide species are typically linear; e.g., see refs 17 and 18. From the spectra, it is clear that ZnOH has a bent geometry, indicative of a more covalently bonded molecule, in analogy to water. It appears that there is sp^3 hybridization at the oxygen atom in this species. The preference for a bent structure may aid in the enzyme functionality of the ZnOH unit.

The rotational constants measured for the six isotopologues were used to establish 18 moments of inertia, from which an accurate structure for ZnOH was calculated. Two structures were determined, r_0 and $r_m^{(1)}$,[43] using the least-squares routine STRFIT.[44] The $r_m^{(1)}$ structure is considered to be more accurate than the r_0 one because it considers zero-point energy changes and thus, is closer to the equilibrium geometry.[43] In Table 3, the structures for ZnOH are listed. As can be seen, the $r_m^{(1)}$ Zn−O and O−H bond lengths are 1.795(1) and 0.967(3) Å, respectively, and the bond angle is θ(Zn−O−H) = 114.2(2)°. These values are quite close to the structure calculated by Trachtman et al.,[32] who predicted r(Zn−O) = 1.817 and r(O−H) = 0.962 Å, with a θ(Zn−O−H) = 114.9°.

As shown in Table 3, the Zn−O−H bond angle (114.2°) is about 10° larger than that of the most fundamental hydroxide species, H_2O, where θ(H−O−H) = 104.5°. The opening of the angle in ZnOH compared to water is likely a result of steric hindrance, caused by substitution of the hydrogen with a much larger metal atom. In CuOH, the angle is 110.1°—about 4° smaller but roughly similar to ZnOH. The ZnOH angle may be slightly larger than that in CuOH because of the presence of the unpaired electron on zinc. (CuOH is closed-shell.) Both bond angles, however, are close to the tetrahedral angle of 109.5°. In contrast, the earlier 3d metals (Ti−Ni) are predicted to have bond angles ranging from ∼116 to 155°,[32] while ScOH is thought to be linear, in analogy to YOH.[27] It is interesting that most enzyme structures containing the ZnOH unit assume a bent geometry; e.g., see ref 4.

Also listed in Table 3 are bond lengths of similar molecules. The O−H bond length in ZnOH, r = 0.967 Å, lies between that

dx.doi.org/10.1021/jp209875a | J. Phys. Chem. A 2012, 116, 1542−1550

of OH^- (r = 0.9643 Å)[45] and H_2O (r = 0.9578 Å),[46] and is comparable to those of AgOH and CuOH[47] (see Table 3). The O−H bond distance in linear YOH is noticeably shorter at r = 0.921 Å.[27] Moreover, the M−O bond lengths in CuOH and ZnOH increase by 0.05−0.1 Å relative to their respective metal oxide species.[48,40] It is speculated that the longer M−O bond enables the M−O−H bond angle to readjust in order to minimize electrostatic repulsion between the positive charge on the metal and H, leading to greater covalent stabilization.[47]

Structural data for the ZnOH unit in carbonic anhydrase II (CAII), as well as in the model zinc enzyme complexes $Tp^{Cum,Me}$ZnOH and $\{\eta^3$-HB(3-Bu^t-5-Mepz)$_3\}$ZnOH, are additionally presented in Table 3. Both complexes are tripodal ligands, which consist of bulky constituents and are often used as model systems for carbonic anhydrase (see Figure 1). All structures were determined by X-ray crystallography.[49−51] Due to the limitations of this technique, only the Zn−O bond length was determined in these compounds; errors cited are on the order of 0.06 Å. The Zn−O bond length for CAII is r(Zn−O) = 2.05 Å,[49] while those of both $[Tp^{Cum,Me}]$ZnOH and $\{\eta^3$-HB(3-Bu^t-5-Mepz)$_3\}$ZnOH are 1.85 Å .[50,51] Calculations suggest that for $[(NH_3)_3Zn(OH)]^+$, another zinc enzyme model species, r(Zn−O) = 1.854 Å.[14] Mauksch et al. also calculated a ZnOH bond angle of 124.1°,[14] about 10° larger than in the monomer, but in reasonable agreement. The model enzyme systems and monomeric ZnOH therefore have very similar Zn−O bond lengths, within 0.05 Å. The bond distance in CAII is about 0.15−0.25 Å longer, in contrast, suggesting that incorporation into a complete enzyme may slightly adjust the basic ZnOH structure.

From the moments of inertia, the inertial defects, Δ_0, of the ZnOH isotopologues were calculated[52] and are listed in Table 2. The inertial defect is a measure of planarity in a molecule. Its sign and magnitude are indicators of rigidity; Δ_0 would be zero for a rigid planar molecule and negative for a nonplanar molecule. For ZnOH and ZnOD, Δ_0 = 0.1138 uÅ^2 and 0.1519 uÅ^2, respectively. In contrast, water has Δ_0 = 0.0460 uÅ^2.[52] These results suggest that while ZnOH is fairly rigid, it is somewhat more "floppy" than water. This property is reflected in the respective vibrational frequencies and force constants. Theoretical calculations predict ZnOH to have a bending mode at ∼599 cm^{-1} and Zn−O and O−H stretching modes at ∼700 and ∼3700 cm^{-1}, corresponding to force constants of ∼0.3, ∼3, and ∼8 mdyn Å^{-1}, respectively.[32] The vibrational modes of water are 1595, 3657, and 3756 cm^{-1} for the bending mode, symmetric stretch, and antisymmetric stretch,[53] respectively, with force constants of ∼8 mdyn Å^{-1} for the OH stretching modes (symmetric and antisymmentric) and ∼0.7 mdyn Å^{-1} for the bending mode.[54] The bending force constant is considerably less in ZnOH than water.

In the analysis of the spin-rotation parameters, it is interesting to note that ε_{aa} is much smaller than and has an opposite sign to ε_{bb} or ε_{cc}, an effect also seen in some metal−hydrosulfide molecules.[55,56] To first order, however, spin-rotational constants are proportional to their respective rotational constants, and A is much larger than both B and C. This discrepancy indicates that ε_{aa} has a large second-order contribution, described by perturbation theory as[57]

$$\varepsilon_{aa}^{(2)} = -2 \sum_{\alpha'} \frac{\langle X|a\mathbf{L}_z|\alpha'\rangle\langle\alpha'|A\mathbf{L}_z|X\rangle + \langle X|A\mathbf{L}_z|\alpha'\rangle\langle\alpha'|a\mathbf{L}_z|X\rangle}{E_X - E_{\alpha'}} \quad (2)$$

where X and α' are the ground and excited perturbing states, respectively, $\mathbf{L}_z$ is the operator for the z-component of orbital angular momentum, A is the rotational constant, and a is the spin−orbit coupling constant, which can be approximated as the atomic value. The ground-state X^2A' state for ZnOH correlates to a $^2\Sigma$ state in the linear limit with the unpaired electron in a 4s orbital. The three nearest excited states would result from the promotion of this electron to a $4p_y$, $4p_x$, or $4p_z$ orbital and have A′ or A″ symmetry, correlating to Π (A′ and A″) and Σ (A′) states in the linear limit. $\mathbf{L}_z$ transforms as an A′ irreducible representation, and the ground state is A′; therefore, in order for the matrix elements in eq 2 to be nonzero, α' must correspond to an A′ state. In this case, the unpaired electron must also reside in the p_y orbital. As a consequence, eq 2 reduces to[58]

$$\varepsilon_{aa}^{(2)} = \frac{-4aA}{E(A') - E(XA')} \quad (3)$$

Because a for Zn or Zn^+ is positive, the second-order interaction results in a negative value for $\varepsilon_{aa}^{(2)}$, which changes the overall sign of the ε_{aa} constant. Note that $\varepsilon_{bb}^{(2)}$ and $\varepsilon_{cc}^{(2)}$ would be zero, because the former corresponds to an excited state with A′ symmetry and the latter concerns the other excited A″ state where the electron is in the p_x orbital. Therefore, ε_{bb} and ε_{cc} are dominated by first-order, rather than second-order, effects.

The nature of the orbital with the unpaired electron can be characterized by examining the two hyperfine parameters determined in this work. The Fermi contact term, a_F, is a measure of the electron density at the nucleus with the spin, in this case the hydrogen, and therefore is nonzero only if the orbital of the unpaired electron has some s character. For ZnOH, a_F(H) = −4.138(19) MHz; i.e., it is small and negative. In comparison, the Fermi contact constant for the electron on the H atom is 1420 MHz.[59] The value of a_F indicates that there is very little electron density directly at the hydrogen nucleus; furthermore, the negative sign suggests that the main coupling results from "spin polarization"; namely, there is an exchange between the unpaired electron and those in the closed shell on the hydrogen atom, which enables the **I**·**S** interaction to occur.[59] This result is not surprising if the unpaired electron is localized on zinc, far from the hydrogen nucleus. The other hyperfine constant established for ZnOH is small and positive, T_{aa} = 4.176(48) MHz, signifying that the unpaired electron has a nonspherical component along the $\hat{a}$ axis, i.e., the axis parallel to the Zn−O bond. The hyperfine constants of ZnOH are thus consistent with the unpaired electron residing principally on the zinc nucleus in an orbital that is not solely 4s in character. Trachtman et al. suggest that the unpaired electron resides in an orbital with sd_σ hybridization.[32]

CONCLUSIONS

The monomeric ZnOH species has been characterized in the gas phase by high-resolution spectroscopy. The spectra of

dx.doi.org/10.1021/jp209875a | J. Phys. Chem. A 2012, 116, 1542−1550

ZnOH and their analysis clearly show that this species has a bent geometry with a near tetrahedral angle, suggesting primarily covalent bonding between the metal atom and the hydroxide ligand. The Zn−O bond length appears to be very similar to what is observed in the ZnOH unit in zinc enzyme model systems. The other metrical parameters determined here may be applicable to these structures. The spin-rotation parameters suggest a nearby A′ excited state. Hyperfine constants indicate that the unpaired electron is in a hybridized orbital on the zinc nucleus. Elucidation of the basic structural and electronic properties of ZnOH will enable a better understanding of the bonding in transition metals and give insight into the role of this unit in enzyme function and surface processes.

■ ASSOCIATED CONTENT

Ⓢ Supporting Information

Table showing observed rotational transitions of the six isotopologues studied. This material is available free of charge via the Internet at http://pubs.acs.org.

■ AUTHOR INFORMATION

Corresponding Author

*E-mail: lziurys@email.arizona.edu. Fax: 520-621-1532.

Present Address

‡Chemistry Department, University of Manitoba, 360 Parker Building, Winnipeg, Canada MB R3T 2N2.

■ ACKNOWLEDGMENTS

This work has been supported by NSF Grant CHE-10-57924. We thank I. Iordanov, A. Taylor, E. Tomat, and H. Vahrenkamp for useful discussions and B. J. Harris for assistance in the laboratory.

■ REFERENCES

(1) Auld, D. Metal Sites in Proteins and Models. In *Structure and Bonding*, Vol. *89*; Hill, H. A. O, Sadler, P. J., Thomson, A. J., Eds.; Springer-Verlag: Berlin, 1997; pp 29−50.

(2) Hedberg, J.; Baldelli, S.; Leygraf, C. *J. Phys. Chem. Lett.* **2010**, *1*, 1679−1682.

(3) Singh., S.; Thiyagarajan, P.; Mohan Kant, K.; Anita, D.; Thirupathiah, S.; Rama, N.; Tiwari, B.; Kottaisamy, M.; Ramachandra Rao, M. S. *J. Phys. D.: Appl. Phys.* **2007**, *40*, 6312−6327.

(4) Christianson, D. W.; Cox, J. D. *Annu. Rev. Biochem.* **1999**, *68*, 33−57 and references therein.

(5) Maret, W.; Li, Y. *Chem. Rev.* **2009**, *109*, 4682−4707 and references therein.

(6) Vahrenkamp, H. *Acc. Chem. Res.* **1999**, *32*, 589−596.

(7) Ibrahim, M. M.; Perez Olmo, C.; Tekeste, T.; Seebacher, J.; He, G.; Maldonado Calvo, J. A.; Bohmerle, K.; Steinfeld, G.; Brombacher, H.; Vahrenkamp, H. *Inorg. Chem.* **2006**, *45*, 7493−7502.

(8) Perez Olmo, C.; Bohmerle, K.; Vahrenkamp, H. *Inorg. Chim. Acta* **2007**, *360*, 1510−1516.

(9) Parkin, G. *Chem. Rev.* **2004**, *104*, 699−768.

(10) Schroder, D.; Schwarz, H.; Schenk, S.; Anders, E. *Angew. Chem., Int. Ed.* **2003**, *42*, 5087−5090.

(11) Díaz, N.; Suárez, D.; Merz, K. M. Jr. *J. Am. Chem. Soc.* **2000**, *122*, 4197−4208.

(12) Merz, K. M. Jr. *J. Mol. Biol.* **1990**, *214*, 799−802.

(13) Silaghi-Dumitrescu, R.; Uta, M.-M.; Kallay, A.; Bodis, J. *J. Mol. Struct.* **2010**, *942*, 15−18.

(14) Mauksch, M.; Brauer, M.; Weston, J.; Anders, E. *ChemBioChem* **2001**, *2*, 190−198.

(15) Kolyagin, Yu. G.; Ordomsky, V. V.; Khimyak, Y. Z.; Rebrov, A. I.; Fajula, F.; Ivanova, I. I. *J. Catal.* **2006**, *238*, 122−133.

(16) Valange, S.; Onida, B.; Geobaldo, F.; Garrone, E.; Gabelica, Z. *Stud. Surf. Sci. Catal.* **2002**, *142*, 215−222.

(17) Anderson, M. A.; Allen, M. D.; Barclay, W. L. Jr.; Ziurys, L. M. *Chem. Phys. Lett.* **1993**, *205*, 415−422.

(18) Anderson, M. A; Barclay, W. L. Jr.; Ziurys, L. M. *Chem. Phys. Lett.* **1992**, *196*, 166−172.

(19) Apponi, A. J.; Barclay, W. L. Jr.; Ziurys, L. M. *Astrophys. J.* **1993**, *414*, L129−L132.

(20) Barclay, W. L. Jr.; Anderson, M. A; Ziurys, L. M. *Chem. Phys. Lett.* **1992**, *196*, 225−232.

(21) Higgins, K. J.; Freund, S. M.; Klemperer, W.; Apponi, A. J.; Ziurys, L. M. *J. Chem. Phys.* **2004**, *121*, 11715−11730.

(22) Ziurys, L. M.; Barclay, W. L. Jr.; Anderson, M. A. *Astrophys. J.* **1992**, *384*, L63−L66.

(23) Bernath, P. F.; Kinsey-Nielsen, S. *Chem. Phys. Lett.* **1984**, *105*, 663−666.

(24) Bernath, P. F.; Brazier, C. R. *Astrophys. J.* **1985**, *288*, 373−376.

(25) Lakin, N. M.; Varberg, T. D.; Brown, J. M. *J. Mol. Spectrosc.* **1997**, *183*, 34−41.

(26) Cannavò, D.; Knopp, G.; Radi, P.; Beaud, P.; Tulej, M.; Bodek, P.; Gerber, T.; Wokaun, A. *J. Mol. Struct.* **2006**, *782*, 67−72.

(27) Adam, A. G.; Athanassenas, K.; Gillett, D. A.; Kingston, C. T.; Merer, A. J.; Peers, J. R. D.; Rixon, S. J. *J. Mol. Spectrosc.* **1999**, *196*, 45−69.

(28) Whitham, C. J.; Ozeki, H.; Saito, S. *J. Chem. Phys.* **1999**, *110*, 11109−11112.

(29) Kauffman, J. W.; Hauge, R. H.; Margrave, J. L. *J. Phys. Chem.* **1985**, *89*, 3541−3547.

(30) Kauffman, J. W.; Hauge, R. H.; Margrave, J. L. *J. Phys. Chem.* **1985**, *89*, 3547−3552.

(31) Wang, X.; Andrews, L. *J. Phys. Chem. A* **2006**, *110*, 10035−10045.

(32) Trachtman, M.; Markham, G. D.; Glusker, J. P.; George, P.; Bock, C. W. *Inorg. Chem.* **2001**, *40*, 4230−4241.

(33) Magnusson, E.; Moriarty, N. W. *Inorg. Chem.* **1996**, *35*, 5711−5719.

(34) Ziurys, L. M.; Barclay, W. L. Jr.; Anderson, M. A.; Fletcher, D. A.; Lamb, J. W. *Rev. Sci. Instrum.* **1994**, *65*, 1517−1522.

(35) Sun, M.; Apponi, A. J.; Ziurys, L. M. *J. Chem. Phys.* **2009**, *130*, No. 034309.

(36) Balle, T. J.; Flygare, W. *Rev. Sci. Instrum.* **1981**, *52*, 33−45.

(37) Sun, M.; Halfen, D. T.; Min, J.; Harris, B.; Clouthier, D. J.; Ziurys, L. M. *J. Chem. Phys.* **2010**, *133*, No. 174301.

(38) Flory, M. A.; McLamarrah, S. K.; Ziurys, L. M. *J. Chem. Phys.* **2006**, *125*, No. 194304.

(39) Tenenbaum, E. D.; Flory, M. A.; Pulliam, R.; Ziurys, L. M. *J. Mol. Spectrosc.* **2007**, *244*, 153−159.

(40) Zack, L. N.; Pulliam, R. L.; Ziurys, L. M. *J. Mol. Spectrosc.* **2009**, *256*, 186−191.

(41) Pickett, H. M. *J. Mol. Spectrosc.* **1991**, *148*, 371−377.

(42) Watson, J, K. G. In *Vibrational Spectra and Structure*; Durig, J. R., Ed.; Elsevier: Amsterdam, 1977; Vol. *6*, pp 1−89.

(43) Watson, J. K. G.; Roytburg, A.; Ulrich, W. *J. Mol. Spectrosc.* **1999**, *196*, 102−119.

(44) Kisiel, Z. *J. Mol. Spectrosc.* **2003**, *218*, 58−67.

(45) Rosenbaum, N. H.; Owrutsky, J. C.; Tack, L. M.; Saykally, R. J. *J. Chem. Phys.* **1986**, *84*, 5308−5313.

(46) Jensen, P.; Tashkun, S. A.; Tyuterev, Vl. G. *J. Mol. Spectrosc.* **1994**, *168*, 271−289.

(47) Whitham, J. W.; Ozeki, H.; Saito, S. *J. Chem. Phys.* **2000**, *112*, 641−646.

(48) Steimle, T.; Namiki, K.; Saito, S. *J. Chem. Phys.* **1997**, *107*, 6109−6113.

(49) Hakansson, K.; Carlsson, M.; Svensson, L. A.; Liljas, A. *J. Mol. Biol.* **1992**, *227*, 1192−1204.

(50) Ruf, M.; Vahrenkamp, H. *Inorg. Chem.* **1996**, *35*, 6571−6578.

(51) Alsfasser, R.; Swiatosloaw, T.; Looney, A.; Parkin, G.; Vahrenkamp, H. *Inorg. Chem.* **1991**, *30*, 4098−4100.

(52) Watson, J. K. G. *J. Chem. Phys.* **1993**, *98*, 5302−5309.

(53) Shimanouchi, T. *Tables of Molecular Vibrational Frequencies Consolidated*, Vol. *I*; National Bureau of Standards: Washington, DC, USA, 1972.
(54) Gordy, W., Cook, R. L. *Microwave Molecular Spectra*; John Wiley & Sons: New York, 1975.
(55) Taleb-Bendiab, A.; Scappini, F.; Amano, T.; Watson, J. K. G. *J. Chem. Phys.* **1996**, *104*, 7431−7436.
(56) Taleb-Bendiab, A.; Chomiak, D. *Chem. Phys. Lett.* **2001**, *334*, 195−199.
(57) Liu, X.; Foster, S. C.; Williamson, J. M.; Yu, L.; Miller, T. A. *Mol. Phys.* **1990**, *69*, 357−367.
(58) Morbi, Z.; Zhao, C.; Bernath, P. F. *J. Phys. Chem.* **1997**, *106*, 4860−4868.
(59) Weltner, W., Jr. *Magnetic Atoms and Molecules*; Van Nostrand Reinhold: New York, 1983.